Title: Spectroscopic and structural investigations of blue afwillite from Ma'ale Adummim locality, Palestinian Autonomy

Author: Rafał Juroszek, Maria Czaja, Radosław Lisiecki, Biljana Krüger, Barbara Hachuła, Irina Galuskina

Citation style: Juroszek Rafał, Czaja Maria, Lisiecki Radosław, Krüger Biljana, Hachuła Barbara, Galuskina Irina. (2020). Spectroscopic and structural investigations of blue afwillite from Ma'ale Adummim locality, Palestinian Autonomy. "Spectrochimica Acta. Part A: Molecular and Biomolecular Spectroscopy" (Vol. 227 (2020), art. no. 117688, s. 1-11), doi 10.1016/j.saa.2019.117688

Spectrochimica Acta Part A: Molecular and Biomolecular Spectroscopy 227 (2020) 117688

Contents lists available at ScienceDirect

Spectrochimica Acta Part A: Molecular and Biomolecular Spectroscopy

journal homepage: www.elsevier.com/locate/saa

Spectroscopic and structural investigations of blue afwillite from Ma'ale Adummim locality, Palestinian Autonomy

Rafał Juroszek [a,*], Maria Czaja [a], Radosław Lisiecki [b], Biljana Krüger [c], Barbara Hachuła [d], Irina Galuskina [a]

[a] Institute of Earth Sciences, Faculty of Natural Sciences, University of Silesia, Będzińska 60, 41-205, Sosnowiec, Poland
[b] Institute of Low Temperature and Structure Research Polish Academy of Sciences, Okólna 2, 50-422, Wrocław, Poland
[c] University of Innsbruck, Institute of Mineralogy and Petrography, Innrain 52, 6020, Innsbruck, Austria
[d] Institute of Chemistry, University of Silesia, Szkolna 9, 40-006, Katowice, Poland

ARTICLE INFO

Article history:
Received 30 August 2019
Received in revised form
9 October 2019
Accepted 21 October 2019
Available online 25 October 2019

Keywords:
Afwillite
Crystal structure
Raman/IR spectroscopy
Luminescence
SiO_3^- hole centre

ABSTRACT

Until now, only the colourless crystals of mineral afwillite, $Ca_3(HSiO_4)_2 \cdot 2H_2O$, were known from several localities around the world. Present work focuses on blue afwillite counterparts from the Ma'ale Adummim locality in Palestine. Using the wide spectrum of analytical methods we attempted to identify the causes of this unusual colour. Structural investigation confirms the presence of two tetrahedral SiO_3OH units connected by hydrogen bonds. The Raman spectrum of afwillite, obtained for the first time, shows the increased number of bands in the range of 785-970 cm^{-1}, whose assignation was correlated with the presence of two different kinds of structural units: $(SiO_3OH)^{3-}$ and its deprotonated counterpart $(SiO_4)^{4-}$. The heating process at 250 °C, in addition to the colour changes from blue to pastel green, shows the intensity reduction and disappearing of some Raman bands attributed mainly to SiO_3OH units. The IR investigation confirms also the presence of that unit and provides information that the position and designation of infrared bands above ~2300 cm^{-1} is related to the strength of hydrogen bonds within the structure. The stretching and bending OH vibrations of afwillite sample show the partial shift to the lower spectral frequencies after the H/D isotopic exchange in OH or H_2O groups. Based on the results of the electron absorption and luminescence analyses it has been proposed that the blue colour of afwillite is caused by hole oxygen defect, most probably SiO_3^-.

1. Introduction

Mineral afwillite, ideally $Ca_3(HSiO_4)_2 \cdot 2H_2O$, is a low temperature hydrated calcium silicate known from several localities around the world [1–5]. For the first time, it was described in association with natrolite, calcite and apophyllite in a dolerite inclusion within kimberlite in the Dutoitspan Mine, Kimberley, South Africa [1]. Based on X-ray diffraction techniques, Megaw [6] and later Malik and Jeffery [7] determined its crystal structure. Both works confirmed the presence of O^{2-}, OH^- ions, as well as neutral H_2O molecules, in the monoclinic structure of afwillite. In turn, the structure of afwillite from the Northern Baikal region investigated by Rastsvetaeva et al. [4] was refined in a triclinic unit cell, which is characterized by a smaller *c* parameter and β angle in comparison to the monoclinic one determined earlier.

As hydrated calcium silicate, afwillite is one of the compounds which can be found in set cement and concrete [8–10]. According to laboratory investigation, afwillite is generally stable in Ca-rich environment and at temperatures below 200 °C [3]. It loses water after heating above 300 °C and can be transformed into the high-temperature mineral rankinite $Ca_3Si_2O_7$ above 1000 °C [8]. Whereas, Tilley [11] suggests that afwillite being a derivative of spurrite $Ca_5(SiO_4)_2(CO_3)$, because of the chemical relationship and close association of these minerals. Afwillite was also synthesized under saturated water pressure in a temperature range of 110-160 °C [12].

The present work is especially focused on the characterization of mineral afwillite from Ma'ale Adummim locality (Palestinian Autonomy) by micro- and spectroscopic techniques. The main aim of the research is to determine the cause of the blue colour of afwillite crystals, which is a unique feature for this phase and was noticed for the first time in the natural specimens. Using a wide spectrum of analytical methods allowed to solve the research problem and receive substantive results. Some of them, like Raman spectrum with the detailed description of vibrational bands or the electron

* Corresponding author.
E-mail address: rjuroszek@us.edu.pl (R. Juroszek).

https://doi.org/10.1016/j.saa.2019.117688

absorption and luminescence spectra of afwillite, were described herein for the first time and allowed to complete the spectroscopic study. Moreover, the obtained results presented in this paper for blue afwillite crystals, along with their detailed analyses, were compared and discussed with previously reported data on the colourless counterpart.

2. Material and methods

2.1. Sample preparation

Rock samples with blue afwillite were collected from the outcrop of the pyrometamorphic Hatrurim Complex in Ma'ale Adummim locality (Palestinian Autonomy) during fieldworks in 2015. The abundance amount of afwillite crystals allowed us to perform various investigations. Several dozen of afwillite crystals were extracted from rock samples. A few of them were prepared for single-crystal X-ray diffraction (SC-XRD) analyses, and the rest were embedded in epoxy and polished. The obtained mount with afwillite crystals was used for scanning electron microscopy (SEM) and electron microprobe analyses (EMPA). Crystals of afwillite were also glued to carbon discs and used in Raman spectroscopy investigation. The next portion of crystals was selected and crushed in a mortar. The powdered samples were prepared for infrared (IR), electron absorption and luminescence spectroscopy and for deuteration process. One thin section was extracted from a rock sample to recognize a mineral association.

2.2. Scanning electron microscopy (SEM) and electron microprobe analysis (EMPA)

The preliminary chemical composition, and crystal morphology of afwillite, as well as associated minerals, were examined using an analytical scanning electron microscope Phenom XL equipped with an EDS (energy-dispersive X-ray spectroscopy) detector (Institute of Earth Sciences, Faculty of Natural Sciences, University of Silesia, Poland).

Quantitative chemical analyses of afwillite were carried out on CAMECA SX100 electron-microprobe apparatus operating in WDS (wavelength dispersive X-ray spectroscopy) mode (Institute of Geochemistry, Mineralogy and Petrology, University of Warsaw, Poland) at 15 kV and 10 nA, beam size ~15 μm. The following lines and standards were used: Ca$K\alpha$, Si$K\alpha$, Mg$K\alpha$ – diopside; Na$K\alpha$ – albite, Al$K\alpha$, K$K\alpha$ – orthoclase; Mn$K\alpha$ – rhodonite; Fe$K\alpha$ – Fe_2O_3.

2.3. Single crystal X-Ray diffraction (SC-XRD)

A single-crystal X-ray diffraction study of afwillite was carried out at ambient condition using a Rigaku OD Gemini-R Ultra diffractometer with Mo$K\alpha$ radiation ($\lambda = 0.71073$ Å) (Institute of Mineralogy and Petrography, University of Innsbruck, Austria). The data reduction was performed with CrysAlisPro (Rigaku 2016). The crystal structure was refined with Jana2006 [13] to an agreement index $R_1 = 2.7\%$, starting from the structural model of the afwillite from type locality – Dutoitspan mine, Kimberly in South Africa, reported by Malik and Jeffery [7]. All of the atoms, except H, were described using anisotropic displacement parameters. Moreover, all H-sites were located by difference Fourier analyses. For refinement of OH bonds and water molecules, distance and angle restraints 1 (0.001) Å, and 109,47 (0.01)° were used.

Further details of data collection and crystal structure refinement are reported in Table 1. Atom coordinates (*x*,*y*,*z*), occupancies, and equivalent isotropic displacement parameters (U_{iso}, Å^2) (Table S1), as well as, anisotropic displacement parameters (Å^2) (Table S2) for blue afwillite crystals are reported in Supplementary Materials.

2.4. Confocal Raman (CR) and infrared (IR) spectroscopy

All spectroscopic measurements were performed at room temperature (~21 °C) for natural afwillite (unheated) and at temperature ~250 °C for heated samples. The temperature experiment allowed checking how do high-temperature influences to water molecules and hydroxyl group.

The Raman spectrum of natural (unheated) and heated afwillite made in the same crystal orientation, was recorded on a WITec alpha 300R Confocal Raman Microscope (Institute of Physics, University of Silesia, Poland) equipped with an air-cooled solid laser 532 nm, 30 mW on the sample and a CCD (closed-circuit display) camera operating at -61 °C. The laser radiation was coupled to a microscope through a single-mode optical fibre with a diameter of 50 μm. An air Zeiss (LD EC Epiplan-Neofluan DIC–100/0.75NA) objective was used. The scattered light was focused on multi-mode fiber (100 μm diameter) and monochromator with a 600 line/mm grating. Raman spectra were accumulated by 20 scans with an integration time of 10 s and a resolution of 3 cm^{-1}. The monochromator was calibrated using the Raman scattering line of a silicon plate (520.7 cm^{-1}). The baseline correction and cosmic ray removal were conducted using WitecProjectFour software, while the peak fitting analysis was performed using the Spectracalc software package GRAMS (Galactic Industries Corporation, NH, USA).

Attenuated total Reflection-Fourier transform infrared (ATR-FTIR) spectra of unheated and heated afwillite were obtained using Nicolet iS10 Mid FT-IR Spectrometer (Thermo Scientific) fitted with an ATR device with a diamond crystal plate (Institute of Earth Sciences, Faculty of Natural Sciences,University of Silesia, Poland). The sample was placed directly on the diamond crystal prior to data acquisition. Measurement conditions were as follows: spectral range 4000-400 cm^{-1}, spectral resolution 8 cm^{-1}, beam splitter Ge/KBr, detector DLaTGS with dynamic interferometer justification. The OMNIC 9 (Thermo Fisher Scientific Inc.) analytical software was used.

In addition, the FTIR spectra of natural and deuterated afwillite were recorded on a Thermo Scientific Nicolet iS50 FTIR spectrometer equipped with a diamond iS50-ATR accessory (Institute of Chemistry, University of Silesia, Poland) in the frequency range of 4000–400 cm^{-1}.

2.5. Deuteration

The deuterated afwillite was obtained by the heating of afwillite solution in heavy water, performed in a pressure reactor (150 °C, 24 h) (Institute of Chemistry, University of Silesia, Poland). The solvent was removed under vacuum at temperature 60 °C in a rotary evaporator (Rotavapor R-100, BÜCHI). The degree of deuterium substitution in afwillite sample was ca. 60–70%.

2.6. Electron absorption and luminescence spectroscopy

The reflectance absorption spectra of powder samples were measured with the Varian Cary 5E UV–Vis-NIR spectrophotometer. Emission spectra were recorded employing FLS980 fluorescence spectrometer from Edinburgh Instrument equipped with a 450 W xenon lamp as an excitation source and a Hamamatsu 928 PMT detector. Emission monochromator was in the Czerny Turner configuration (1800 lines per mm holographic grating blazed at 300 nm, 0.2 nm resolution). Measured spectra were corrected for the sensitivity and wavelength of the experimental setup. To record some luminescence spectra and adequate decay curves a femtosecond laser (Coherent Model "Libra") that delivers a train of 89 fs pulses at a wavelength of 800 nm and pulse energy of 1 mJ with a repetition rate-regulated up to 1 kHz was applied as an excitation

source. To attain light pulses at different wavelengths (230–2800 nm) the laser is coupled to an optical parametric amplifier (Light Conversion Model OPerA). Luminescence decay curves were recorded with a grating spectrograph (Princeton Instr. Model Acton 2500i) coupled to a streak camera (Hamamatsu Model C5680). All measurements were performed at room temperature (T = 293 K).

3. Results and discussion

3.1. Occurrence, physical properties and mineral association

The rock samples with blue afwillite crystals were found and collected in Ma'ale Adummim locality in the Judean Desert, 8 km east of Jerusalem in Palestinian Autonomy. This place is a part of the large pyrometamorphic Hatrurim Complex (or the Mottled Zone) distributed on both sides of the Dead Sea Transform Fault [14–20]. The uniqueness of this Complex is related to new mineral discoveries [21–28]. In these samples composed mainly, by cuspidine, gehlenite and flamite, afwillite occurs together with ettringite, thaumasite, Cr^{3+}-bearing ettringite, calcite, minerals of baryte-hashemite solid solution and undiagnosed Ca-hydro silicate with a pearly lustre (Fig. 1). The phases listed above form low-temperature hydrothermal assemblages, which filled cavities and fissures, and also cover the crack surface in pyrometamorphic rocks (Fig. 1).

Afwillite from Ma'ale Adummim specimen is transparent with a vitreous lustre. The light-blue colour of crystals is the most interesting and uncommon feature of this mineral (Fig. 1a,c,e). Hitherto, only transparent and colourless afwillite crystals were described from several localities around the world [1–3]. Afwillite forms characteristic radial-spherical aggregates (3 mm in diameter) which consist of elongated tabular crystals up to 1 mm long (Fig. 1a–f). Prismatic ettringite crystals with characteristic and distinct colour zonation are noted on the surfaces of these spheres (Fig. 1c). The difference in colour is connected to the gradual substitution of Al^{3+} by Cr^{3+} within the structure of this mineral. Spherical-aggregates are formed by intergrowing aggregates of afwillite, ettringite and minerals of the baryte-hashemite series (Fig. 1e–f).

Table 1
Parameters for X-ray data collection and crystal-structure refinement for afwillite.

Crystal data	
Refined chemical formula sum	$Ca_3Si_2O_{10}H_6$
Crystal system	Monoclinic
Space group	*Cc* (No. 9)
Unit-cell dimensions	$a = 16.250(5)$ Å $b = 5.6227(5)$ Å $c = 13.209(4)$ Å $\alpha = \gamma = 90°$, $\beta = 134.84°$
Volume	855.8 (8) Å^3
Formula weight	342.5
Density (calculated)	2.659 g/cm^3
Z	4
Data collection	
Crystal shape	tabular
Temperature	293
Diffractometer	four-circle diffractometer Xcalibur, Ruby, Gemini ultra
X-Ray radiation	Mo$K\alpha = 0.71073$ Å
Monochromator	Graphite
min. & max. theta	3.54, 29.4
Reflection ranges	$-22 \le h \le 21$ $-5 \le k \le 7$ $-16 \le l \le 14$
Refinement of structure	
Reflection measured	1883
No. of unique reflections	1359
No. of observed unique refl. $I > 3/s(I)$	1325
Refined parameters	160
R_{int}	0.0233
R_1	0.0270
GooF	1.68
$\Delta_{\rho min}$ [e Å^{-3}]	-0.62
$\Delta_{\rho max}$ [e Å^{-3}]	0.40

3.2. Mineral chemistry

Chemical analyses presented in Table 2 indicate that afwillite from Ma'ale Adummim locality is chemically homogenous. The amount of all impurities, like Na, K, Fe, Mg, and Mn was below the detection limit of the microprobe analyses. The empirical formula calculated on 5 cations is as follows: $Ca_{3.01}(HSi_{1.99}O_4)_2 \cdot 2H_2O$.

The results obtained from the EMPA analyses are in good agreement with the literature data. We observed that the mass % of main constituents (SiO_2 and CaO) are very similar to afwillite chemical composition from the Kimberly mine in South Africa [1], Crestmore in California [2] and Fuka in Japan [3]. At the mentioned localities, the content of the main components ranges within 33.96-34.76 and 48.35–49.28 for SiO_2 and CaO, respectively. Moreover, the minor fluorine content was detected in the chemical composition of afwillite from Crestmore [2], as well as in afwillite from Fuka, in the composition of which, besides fluorine also B impurity is present [3].

3.3. Crystal structure of afwillite from Ma'ale Adummim locality

The crystal structure of blue afwillite from Ma'ale Adummim was refined in a monoclinic unit cell with the following parameters $a = 16.250(5)$ Å, $b = 5.6227(5)$ Å, $c = 13.209(4)$ Å, $\alpha = \gamma = 90°$, $\beta = 134°84'$, $V = 855.8(8)$ Å^3. The crystal structure shown in Fig. 2 is composed of the double chains of calcium polyhedra, which are connected through the corners and edges with isolated silicon tetrahedra. Structural investigation allows us to recognize three types of seven coordinated calcium polyhedra and two types of silicon tetrahedra. Moreover, O^{2-}, OH^- and H_2O groups were distinguished within the crystal structure. According to bond valence calculation, we identified O2 and O4 atom as OH^-, O5-O8 as O^{2-} and O9-O10 as H_2O groups. Like Megaw [6], and also Malik and Jeffery [7], we determined O1 and O3 as oxygen, not as a hydroxyl group.

The interatomic distances between cation-oxygen are given in Table 3. Most of the Ca-O distances are in the range 2.316(6)-2.556(5) Å, but in Ca2 and Ca3 atoms, there are four significantly longer bonds (two in each) which have changing distances from 2.778(5) Å to 2.871(5) Å, and from 2.704(7) Å to 2.737(5) Å, respectively. The similar remark was noted by Malik and Jeffery [7] in previously reported structural data.

Each silicon atom in afwillite structure is surrounded by three oxygen and one hydroxyl group, which form together tetrahedral arrangement as SiO_3OH unit. These two types of silicon tetrahedra do not share any corners or edges but are interconnected by hydrogen bonds.

The $Si1O_4$ tetrahedron shares one edge with $Ca1O_7$ polyhedron between O7-O8 oxygen atoms, while, the $Si2O_4$ shares two edges with Ca2 and Ca3 polyhedra between O5-O6 and O2-O5, respectively. The length of shared edges (equivalent of the distance between O-O) between Ca-polyhedron and Si-tetrahedron are in the range from 2.590 Å to 2.648 Å and are in good agreement with the same distances in earlier reported structures [6,7]. The average length of unshared edges in tetrahedron is equal to 2.676 Å for $Si1O_4$ and 2.685 Å for $Si2O_4$. The Si-O distances in afwillite structure vary from 1.600(4) to 1.681(7) Å (Table 3), in turn, the tetrahedral O-Si-O angles are in ranges 106.5–116.3° and 103.4–112.8° for $Si1O_4$ and $Si2O_4$ tetrahedron, respectively.

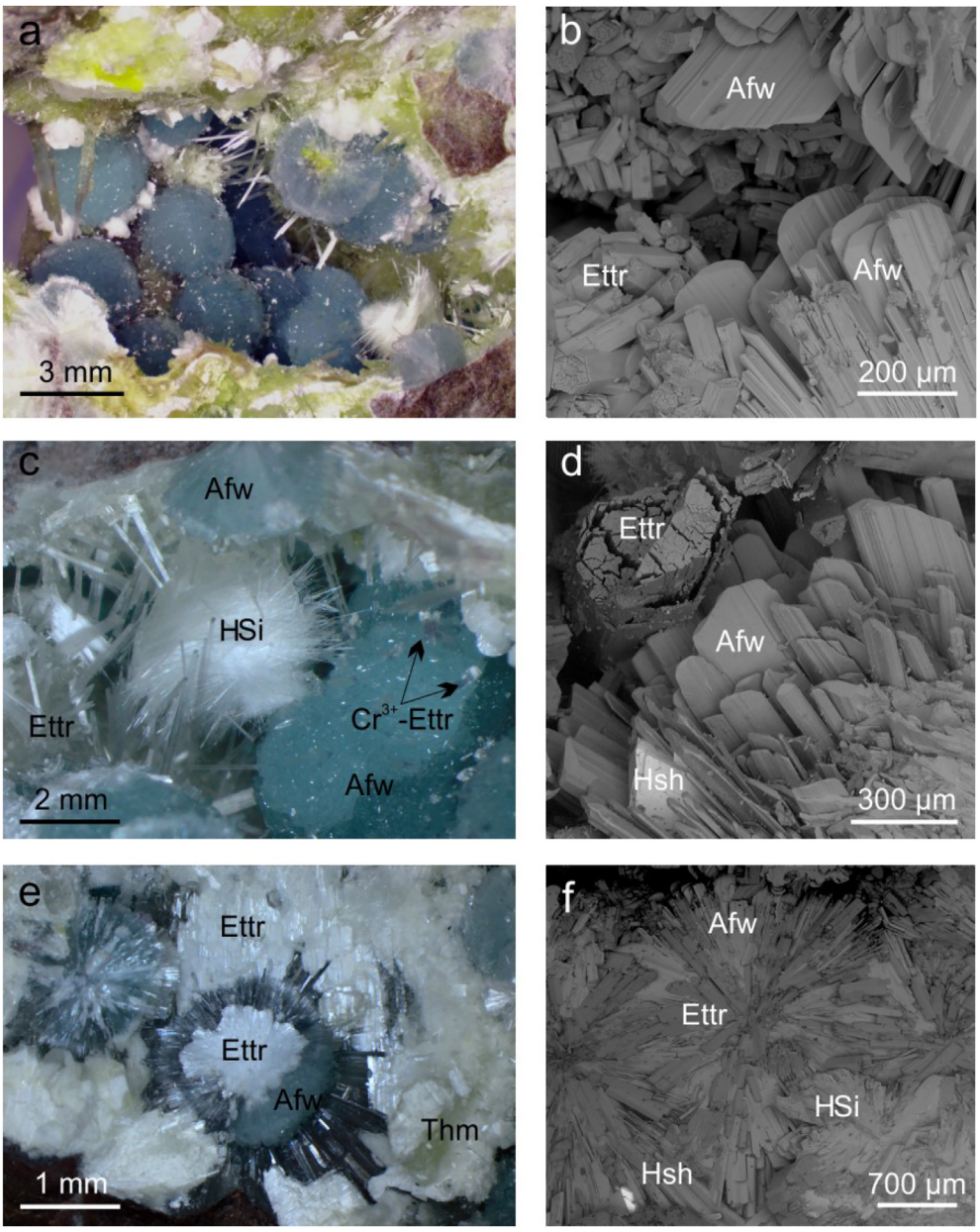

Fig. 1. Macroscopic and BSE (backscattered electron) images of the cavity fragment filled by light-blue spherical aggregates of afwillite and other low-temperature hydrothermal minerals from Ma'ale Adummim locality (a,c). Characteristic tabular morphology of afwillite crystals (b,d). A cross-section of ball-shaped afwillite (e–f). Afw – afwillite; Cr^{3+}-Ettr – Cr^{3+}-bearing ettringite; Ettr – ettringite; Hsh – hashemite; HSi– calcium hydrosilicates; Thm – thaumasite.

The evident differences in terms of bond lengths and angles, as well as the acid character of the Si tetrahedra and the presence of long Si-OH distances between Si1-O4 and Si2-O2 equal to 1.681(7) Å and 1.675(5) Å, causes a considerable distortion of both tetrahedra in the crystal structure of afwillite. The values of tetrahedral mean quadratic elongation (λ) and bond angle variance (σ^2), calculated according to Robinson et al. [29], are $\lambda = 1.0033$ and $\sigma^2 = 14.12$ in $Si1O_4$, and $\lambda = 1.0031$ and $\sigma^2 = 12.22$ in $Si2O_4$.

Table 2
Chemical composition (wt.%) of afwillite from Ma'ale Adummim locality.

Constituent	Mean	S.D.	Range
	n = 20		
SiO_2	34.88	0.26	33.73–34.59
CaO	49.12	0.36	48.66–49.61
H_2O[a]	15.75		
Total	99.75		
Calculated on the basis of 5 cations			
Si^{4+}	1.99		
Ca^{2+}	3.01		

[a] Water was calculated on the basis of stoichiometry; S.D. = 1σ – standard deviation; n – number of analyses.

A hydrogen bonding arrangement has a significant contribution to the stability of the afwillite structure. The geometry of hydrogen bonds determined during the structural investigation of blue afwillite crystals, as well as characteristic donor-acceptor distances and angles are summarized in Table 4. According to the *d*(O-O) distances [30], we may favour four strong hydrogen bonds, in which these distances are in the range 2.5-2.7 Å. They are related for configuration between the hydroxyl group and oxygen (O2–H2···O1, O4–H4···O3) or water molecules and oxygen (O9–H9b···O3 and O10–H10b···O1). The weak hydrogen bonds with *d*(O-O) > 2.70 Å are assigned to O9–H9a···O10 and O10–H10a···O4 configurations.

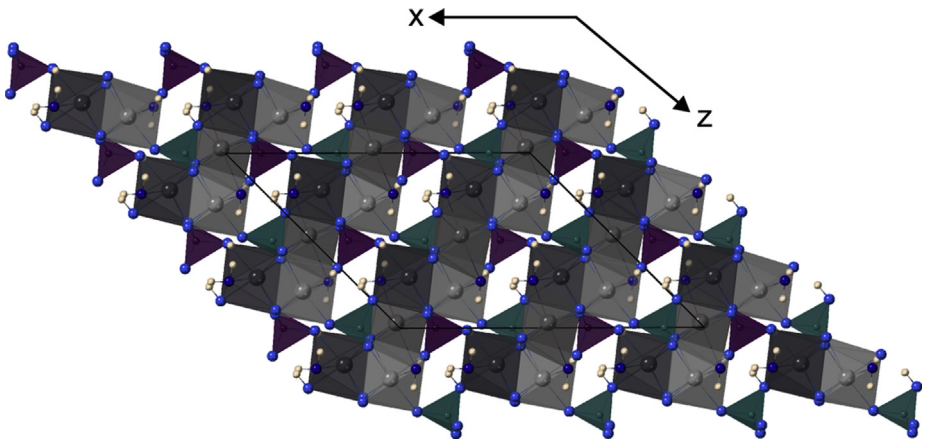

Fig. 2. Crystal structure of blue afwillite from Ma'ale Adummim projected along (010). Three types of calcium atoms (Ca1-Ca3) are presented as grey polyhedra, two types of SiO_4 tetrahedra are in purple (Si1) and green (Si2). The oxygen atom, as well as water molecules and hydrogen atoms, are shown as blue, dark blue and light-brown spheres, respectively.

Table 3
Interatomic cation-oxygen distances (Å) in the blue afwillite crystal structure.

Symbol	Ca1	Ca2	Ca3	Si1	Si2
O1	–	2.350(6)	–	1.611(5)	–
O2	2.414(6)	–	2.737(5)	–	1.675(5)
O3	–	2.316(6)	–	–	1.626(7)
O4	2.465(6)	–	–	1.681(7)	–
O5	2.351(4)	2.323(5)	2.347(5)	–	1.626(4)
O6	2.354(5)	2.871(5)	2.337(4)	–	1.600(4)
O7	2.401(5)	2.354(4)	2.343(5)	1.631(4)	–
O8	2.556(5)	2.401(4)	2.354(5)	1.614(4)	–
O9	2.511(5)	–	2.483(6)	–	–
O10	–	2.778(5)	2.704(7)	–	–

Table 4
The geometry of hydrogen bond in afwillite.

Configuration	$d(O_d{-}O_a)$/Å	$d(O_d{-}H)$/Å	$d(H\cdots O_a)$/Å	O–H···O angle (°)
O2–H2···O1	2.570(9)	1.00(8)	1.61(9)	159(5)
O4–H4···O3	2.530(5)	1.00(3)	1.59(4)	154(5)
O9–H9a···O10	2.837(9)	1.00(11)	1.98(11)	142(7)
O9–H9b···O3	2.584(7)	1.00(4)	1.60(4)	167(7)
O10–H10a···O4	2.760(7)	1.00(16)	1.78(3)	164(6)
O10–H10b···O1	2.619(5)	1.00(4)	1.65(3)	162(4)

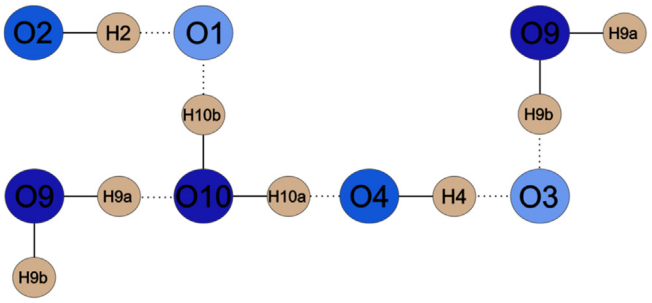

Fig. 3. Schematic diagram of hydrogen bonds in afwillite, modified after Malik and Jeffery [7]. Oxygen atoms are shown as blue (light-blue for O^{2-}, blue for oxygen in OH group and dark blue for oxygen in H_2O) and hydrogen atoms as brown spheres.

In Fig. 3 the schematic diagram of hydrogen bonds in afwillite is shown. This bonding network is comparable with that proposed by Malik and Jeffery [7] and confirms also the nature of water molecules. Moreover, it shows the connection between two water molecules and their linkage with questionable O1 and O3 atoms. The d(O-O) distances between O9-O3 and O10-O1, as well as O–H···O angles are very similar, and vary from 2.584 to 2.619 Å and from 162° to 167°, respectively (Table 4).

Microprobe analyses also confirm a presence of two hydroxyl groups in the crystal chemical formula, the one per each tetrahedron, and two water molecules. Therefore, chemical composition corresponds to the structural, refined composition. It means that the crystal structure should contain 6 hydrogen atoms and 10 oxygen atoms, consequently two OH group and two H_2O molecules take place and the rest of oxygen atoms belonging to the Si tetrahedra. Determination of the position and number of hydrogen atoms is very difficult during the structural investigation, therefore based on electron density distribution we can try to confirm their presence. Rasvetsaeva et al. [4] refined the structure of afwillite from the Northern Baikal region in the triclinic unit cell. They specified in the structure Si tetrahedra containing two OH groups, but only half of them. In other tetrahedra terminal oxygen vertices were involved in donor-acceptor bonds with H_2O and OH groups [4]. They proposed the crystal chemical formula with $[SiO_2(OH)_2]$ and SiO_4 including both types of tetrahedra. Our data refined in the monoclinic system are different, therefore, like other researchers, we classify O1 and O3 as O^{2-} and only O2 and O4 as hydroxyl groups.

3.4. Raman and infrared spectroscopy data

The structural investigation revealed two types of silicon tetrahedra in the crystal structure of blue afwillite. According to the theoretical predictions, the ideal tetrahedral coordination $(SiO_4)^{4-}$ with T_d point group symmetry has nine normal vibrations, which are characterized by four fundamental modes: ν_1 (A) – symmetric stretching vibration, ν_2 (E) – doubly degenerate symmetric bending vibration, ν_3 (F_2) – triply degenerate asymmetric stretching vibration and ν_4 (F_2) – also triply degenerate asymmetric bending vibration [31–33]. In this context, all vibrations are active in Raman spectroscopy, whereas only ν_3 and ν_4 are active in infrared. On the basis of structure refinement of afwillite it was established a presence of $(SiO_3OH)^{3-}$ unit in its structure instead of ideal $(SiO_4)^{4-}$ tetrahedron. In the structure of some minerals belonging to the uranophane and sklodowskite groups, this unit is also observed [31]. As the authors reported, the presence of $(SiO_3OH)^{3-}$ may be explained by a decreasing symmetry of ideal tetrahedral coordination from T_d to C_{3v}, which implicate the local structural re-arrangement, and as a consequence a splitting of individual bands in the spectrum. Moreover, local structural deformation (mutual rotation of tetrahedral units) probably corresponds

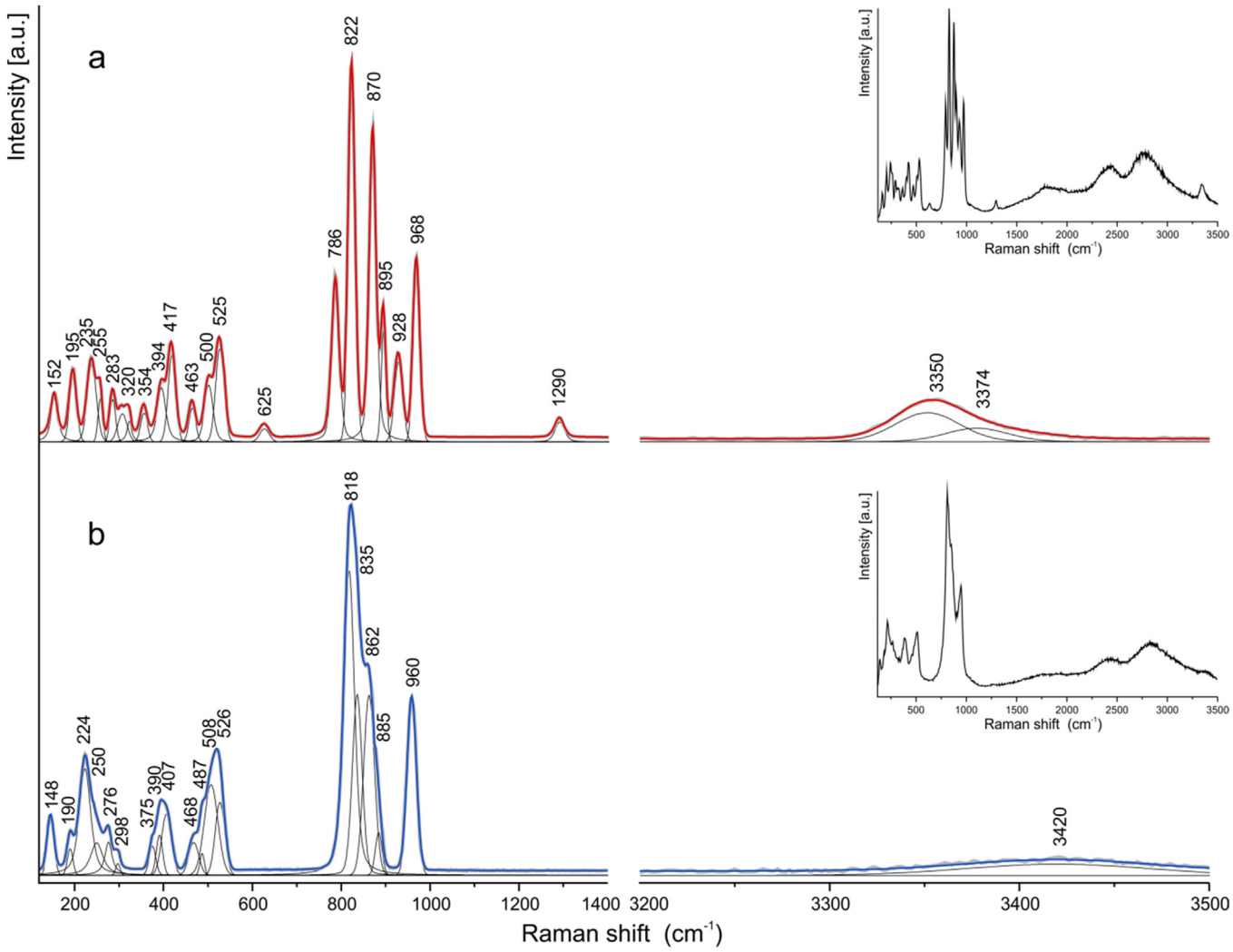

Fig. 4. Raman spectra of natural (unheated, a) and heated (b) blue afwillite.

to the activation of additional stretching and bending vibrations due to the presence of tetrahedral units in two variable surroundings.

The Raman spectrum of unheated afwillite, presented in Fig. 4a revealed bands in the range between 780 and 970 cm^{-1}. A great number of bands and their positions can confirm previously done assumption about structural deformation enforced by protonation of the ideal silica tetrahedron. Another hypothesis explaining observed effects is the presence of two different kinds of structural units: $(SiO_3OH)^{3-}$ and its deprotonated counterpart $(SiO_4)^{4-}$. In both cases, the afwillite structure is probably stabilized by the presence of hydrogen bonds, which determine a character of the Raman spectrum of the mineral. As a result, irrespective of the hypothetical assumptions concerning to the number of $(SiO_3OH)^{3-}$ and $(SiO_4)^{4-}$, an origin of the two strongest bands centred at 822 and 870 cm^{-1} are caused by the symmetric Si-O stretching ν_1 vibrations (Fig. 4a). In turn, the nature of the bands in the range 895-970 cm^{-1} can be related to ν_3 asymmetric stretching vibrations. The nature of bands at 786 cm^{-1} and 1290 cm^{-1} is interesting, in our interpretation they can be assigned to the Si-OH deformation and stretching modes, but the band positions are strictly determined by the character of hydrogen bonds.

In the Raman spectrum of the heated afwillite (Fig. 4b), visible changes are observed in the stretching vibration region in the range 800-960 cm^{-1}. The bands connected with the Si-O symmetric and asymmetric stretching vibration of $(SiO_4)^{4-}$ group are still present in the spectrum at 818 and 960 cm^{-1}, respectively. The positions of these bands are shifted to the lower frequencies in comparison to their positions in the unheated spectrum (Fig. 4a). In turn, the intensity of the bands related to the stretching vibration of $(SiO_3OH)^{3-}$ unit has been reduced and its position was also shifted to the lower wavenumbers, in range 835-885 cm^{-1}. Similarly, the bands at ~930 cm^{-1} and 786 cm^{-1} observed in the unheated spectrum disappeared after heating. It can suggest a weakening of the hydrogen bonds due to the thermal effects.

The low-frequency range in the Raman spectrum of the unheated sample (Fig. 4a) is determined by the presence of many overlapping bands with relatively low intensity. There, the bands in the ranges 390-420 cm^{-1} and 480-530 cm^{-1}, are attributed to the ν_2 and ν_4 bending modes of Si-O-Si in $(SiO_4)^{4-}$ groups (Fig. 4a). The formers may overlap also with the vibration of the Ca-O in octahedral coordination. Other bands observed at 463 and 625 cm^{-1} can be associated with the vibrations in $(SiO_3OH)^{3-}$ unit. It is worth to notice that the assignation of the latter one may be questionable and is also related to the bending Si-OH out-of-plane mode [31]. Raman bands below 320 cm^{-1} are usually ascribed to the lattice vibrations. The spectral region related to the bending vibration also have been regrouped in the Raman spectrum of the heated sample (Fig. 4b), and here only symmetric and asymmetric bending vibrations of $(SiO_4)^{4-}$ group are noted in the 375—417 and ~470-530 cm^{-1} ranges.

Identification of bands in-between the 1500 and 3200 cm^{-1} is problematic in both spectra, but one can assume that their origin can be a result of a fluorescence effect, conditional by a presence of structural defects and the atypical protonated silica tetrahedral units. The bands related to the O-H stretching vibrations in H_2O were observed in the range 3300-3450 cm^{-1} for unheated afwillite (Fig. 4a). For heated afwillite the band shift is also noted, the broad band related to the OH stretching vibration is centred at ~3420 cm^{-1} (Fig. 4b). The presence of the weak and broad band may confirm the hypothesis on reorganization of $(SiO_3OH)^{3-}$ unit and weakening of hydrogen bonds stabilizing the afwillite structure.

The changes observed in the Raman spectra of natural and heated afwillite sample suggest that the presence or absence of some bands may be associated mostly with the vibration of the $(SiO_3OH)^{3-}$ unit. As a result of the heating process, the presence of the proton of such group which in the unheated spectrum probably forms a hydrogen bond system yield to distract due to the temperature and in consequences provide to the disappearance of some bands. The specific band arrangement in the unheated spectrum, especially due to the marker bands at 463, 625, 786, in between 870-930 and 1290 cm^{-1} provide a conclusion about the existence of protonated silica tetrahedral units defined as $(SiO_3OH)^{3-}$ because of the vanishing due to the heating, of the band pattern associated with the vibration within this group.

Afwillite belongs to the orthosilicates (nesosilicates), which contain isolated SiO_4 tetrahedra with T_d symmetry in the structure [34]. Handke and Urban [35] performed Raman investigation for some orthosilicates, in which Raman active symmetric and asymmetric stretching vibrations are in the ranges 820-865 cm^{-1} for ν_1 and 880-978 cm^{-1} for ν_3, respectively. The symmetric stretching vibrations of the Si-O bond in tetrahedra were also observed by many authors, who assigned its to the following positions in the Raman spectra: 850 cm^{-1} [36], 861 cm^{-1} [37], and the 800-950 cm^{-1} range [33]. Griffith [38], using IR and Raman spectroscopy, analysed a dozen orthosilicates belonging to the different mineral groups and showed that the position of both symmetric vibrations is changeful. For example, ν_1 for forsterite is at 823 cm^{-1}, whereas for phenakite at 877 cm^{-1}. Our results on the stretching vibrations of $(SiO_4)^{4-}$ group in afwillite are in good agreement with previously reported data.

Symmetric and asymmetric bending vibrations in orthosilicates according to Handke and Urban [35] are in the ~350-440 cm^{-1} and ~490-610 cm^{-1} ranges, respectively. Griffith [38], as in the case of stretching vibrations, stated that the position of bending modes is distinct and is related to the mineral group. For example, ν_4 in forsterite is at 602 cm^{-1}, whereas in phenakite - at 444 cm^{-1}. The literature data confirmed the correctness of afwillite spectroscopic results of bending vibration assignation.

A tetrahedron consisting of silica surrounding by three oxygens and one hydroxyl group – $(SiO_3OH)^{3-}$, is recognized not only in afwillite structure. It was reported in the structures of some uranyl silicates like uranophane, sklodowskite, boltwoodite [31], bultfonteinite [39], olmiite [40] and poldervaartite [41]. During detailed spectroscopic investigations of uranyl minerals Frost et al. [31] assigned Raman bands in the 900–1150 and 390-570 cm^{-1} ranges to the $(SiO_4)^{4-}$ stretching and bending vibrations, respectively. There are no Raman spectroscopic data on bultfonteinite. In the Raman spectra of olmiite and poldervaartite Si-O symmetric and asymmetric stretching vibrations of $(SiO_3OH)^{3-}$ unit were attributed to bands at ~852 cm^{-1} and ~900-955 cm^{-1}, respectively [42,43]. In our work bands generated by $(SiO_3OH)^{3-}$ unit are shifted to the higher wavenumbers. It can be connected by the presence of two distinct tetrahedra in afwillite structure. In this case, bond length, oxygen position and type of connection causing between tetrahedra and polyhedra case resulting in high distortion, which is confirmed by structural analyses. In studied minerals Frost et al. [31] assigned bands as vibration associated with Si-OH deformation modes in the spectral region ~790-810 cm^{-1}. In unheated afwillite (Fig. 4a) band related to these vibrations at 786 cm^{-1} is very close to this range, which is in keeping with data reported before.

At high wavenumber region situation is more complicated because in the afwillite spectrum we observe only the broad bands placed below ~3400 cm^{-1}. In olmiite and poldervaartite several bands assigned to the OH stretching vibrations of the (SiO_3OH) were reported [42,43]. We suggest that in afwillite this type of vibration is absent because OH^- ion is usually indicated as a sharp band between 3450 and 3700 cm^{-1}. For example, in zeolites bands associated with SiOH stretching vibrations are placed at wavenumbers >3600 cm^{-1} [31]. In Raman spectra of the uranophane group minerals bands in the range 3400-3600 cm^{-1} are assigned to OH stretching vibrations of water molecules. Bands assignation in this spectral region in the Raman spectrum of afwillite is in accordance with the published data.

In the infrared spectrum of unheated afwillite shown in Fig. 5b, strong bands are observed at 860 cm^{-1} and in the range 909-960 cm^{-1}. These bands are attributed to the Si-O symmetric and asymmetric stretching vibrations of $(SiO_3OH)^{3-}$ unit. Other infrared bands noted at 775 cm^{-1} and 810 cm^{-1}, according to the Raman band assignation, can be related to hydroxyl deformation modes. Symmetric and asymmetric bending vibrations connected with SiO_3OH tetrahedra are presented in the infrared spectrum as bands at ~470 cm^{-1} and ~630 cm^{-1}, respectively. The two bands between 1280-1325 cm^{-1} are related to the Si-O vibrations, while the band at 1097 cm^{-1} is associated with the Si-O-Si asymmetric stretching vibrational mode.

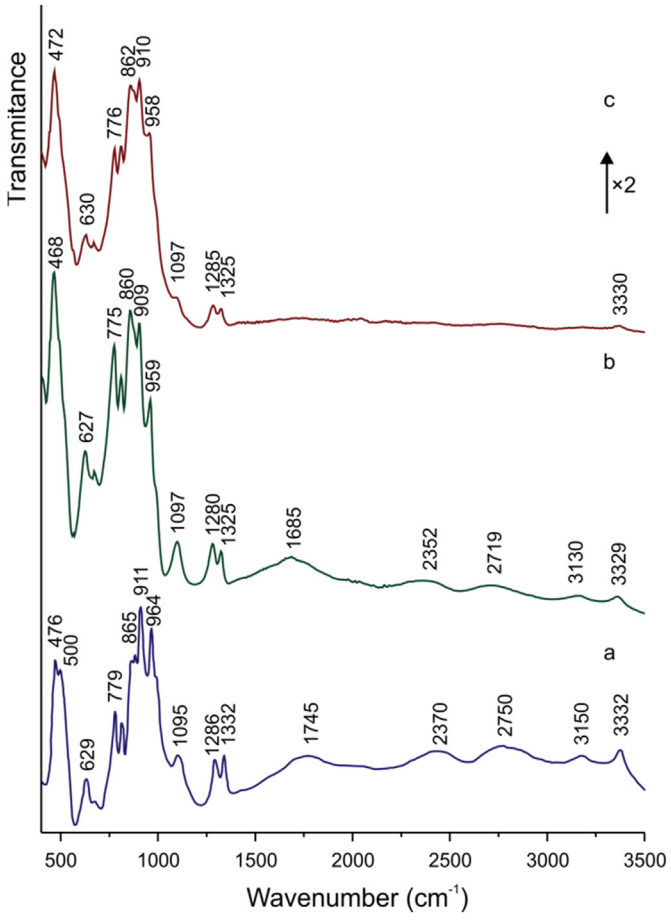

Fig. 5. IR spectra of afwillite from Northern Baikal region (a) and from Ma'ale Adummim locality before (b) and after heating (c).

The infrared spectrum over the 2300 cm^{-1} frequencies contains two very broad absorption bands centred at approximately 2352 and 2719 cm^{-1} and two less broad bands at 3130 and 3329 cm^{-1}. All these bands are attributed to the υ OH stretching vibrations of OH and H_2O groups. The frequencies of the υ OH vibrations depend on the strength of the hydrogen bond. Strong hydrogen bonds, which corresponding to the short O-O distances, are usually related to broad infrared bands in the spectral region 2000-3000 cm^{-1}, whereas weak H-bonds are associated with sharper bands between 3000-3500 cm^{-1} [44]. There are two strong hydrogen bonds between the hydroxyl group and oxygen (O2—H2···O1, O4—H4···O3) in afwillite structure, then it is highly probable, that the bands at 2352 and 2719 cm^{-1} are connected with these strong bonds. In turn, the bands at 3130 and 3329 cm^{-1} can be related to the weak hydrogen bonds forming in the following configurations O10—H10a···O4 and O9—H9a···O10. Summarise, the bands noted <3000 cm^{-1} in the infrared spectrum of afwillite are attributed to the υ OH vibrations of hydroxyl group linked to the Si atom in tetrahedra. In turn, the bands above this frequency are related to the υ OH vibrations of H_2O. In this case, a broad band at 1685 cm^{-1} is connected with the water δ H-O-H bending modes.

Changes in the spectrum of the heated sample are observed in the intensities of bands (Fig. 5). Comparing spectra b and c in Fig. 5 we noted that the spectra below 1325 cm^{-1} look similar and only band at 1097 cm^{-1} has been strongly reduced. The greater changes have been observed above 1500 cm^{-1}. As a result of the heating process hydrogen bonds system has been disturbed and almost all infrared bands disappeared above this frequency. Only one band at 3330 cm^{-1} related to OH vibrations in water can be discerned.

There are a few examples of infrared spectrum of colourless afwillite from different localities around the world in literature: Yoko-Dovyren massif, Buryatia Republic, Transbaikal Territory, Siberia, Russia [4], Crestmore quarry, north of Riverside, Riverside Co., California, USA [45], and Lakargi Mt., Upper-Chegem caldera, Northern Caucasus, Republic of Kabardino-Balkaria, Russia [45]. Despite similarities in the bands' frequencies, only infrared spectrum from the first locality was described so far. For comparison, an adequate spectrum was added to Fig. 5 (a). The assignation of the Si-O stretching vibrations related to the isolated SiO_4 tetrahedra by Rastsvetaeva et al. [4] is comparable with our description. Other bands were assigned in a different way and were correlated with the presence of the hydronium cation H_3O^+ solvated by one water molecule and formed during this process the Zundel complex $H_5O_2^+$ [4].

The infrared spectrum of afwillite sample from Dutoitspan Mine, Kimberley, South Africa [44] has been examined in the region 2000-3500 cm^{-1} to identify of OH stretching vibrations connected with a hydroxyl group and water molecules. Their results are comparable with our prediction and confirmed that the stability of afwillite structure depends on hydrogen bonding system. Moreover, published data suggest that in minerals where Si with three apical O atoms is present, the Si-O-H group with covalent O-H bond can be formed and in the infrared spectrum several bands in region 1300-3200 cm^{-1} appear [31]. The identical feature is noted in the afwillite IR spectrum. Furthermore, the similar frequencies of bands associated with $(SiO_3OH)^{3-}$ unit in afwillite and other minerals like olmiite [42] and poldervaartite [43] and correlation with Raman band assignation, presented herein for the first time, can provide the correct interpretation of spectroscopic data.

Afwillite sample was also investigated using the hydrogen-deuterium exchange of the hydrogen protons by IR spectroscopy technique. FTIR measurements included the natural and deuterated afwillite samples. The absorption area, occurring in the spectral range between 1300 to 400 cm^{-1} in IR spectra of both samples, was omitted for the interpretation due to their similarities, as shown in Fig. 6b. Thus, we focused on the detailed analysis of the bending (Fig. 6a) and the stretching (Fig. 6b) vibration regions attributed to the hydroxyl groups in H_2O units.

The bands in the frequency region of 1400-1800 cm^{-1} were attributed to the O-H bending vibration, designated as δ(H-O-H) (Fig. 6a). Two bands at 1435 cm^{-1} and 1642 cm^{-1} in IR spectrum of natural afwillite (black line) were in a good agreement with the bending modes in IR spectrum of unheated afwillite from Ma'ale Adummim (Fig. 6b), which was represented by the wide band centred at 1685 cm^{-1}. The identification of these two characteristic bands may be associated with measurements conditions or sample quality. The band at 1325 cm^{-1}, as was described earlier, is connected with the Si-O vibrations.

In the IR spectrum of the deuterated sample (red line), the band at 1640 cm^{-1} was almost completely reduced, whereas the peak associated with the O-D bending vibration appeared at lower frequencies at 1437 cm^{-1} with a simultaneous increase of band intensity. In the case of the IR spectrum of natural afwillite (black line in Fig. 6b), a broad band centred at 3366 cm^{-1} was assigned to the O-H stretching vibrations of H_2O groups. The assignment of the vibration frequencies at 2650 cm^{-1} was questionable. It could be correlated with the band at ~2720 cm^{-1} in Fig. 5b and can be ascribed to the strong hydrogen bond between O-H···O units in the crystal structure. Replacement of the hydrogen atoms by deuterium atoms in the hydrogen bridges results in a decrease of the vibrational frequency of the deuteron stretching vibration (relative to the $\nu_{X\text{-}H}$ band) about $\sqrt{2}$ times. As a result of deuteration, some part of the water units has been replaced by D_2O units and their absorption peaks shifted to the lower wavenumber region. Currently, we found the bands at 2510, 2650 and 2692 cm^{-1} (red line in Fig. 6b) which may be ascribed to the stretching vibrations of D_2O and a wide band at 3400 cm^{-1} related to the υ H_2O vibrations.

3.5. The electron absorption and luminescence spectra

The absorption spectra of the natural and heated afwillite sample measured at room temperature are shown in Fig. 7. In the

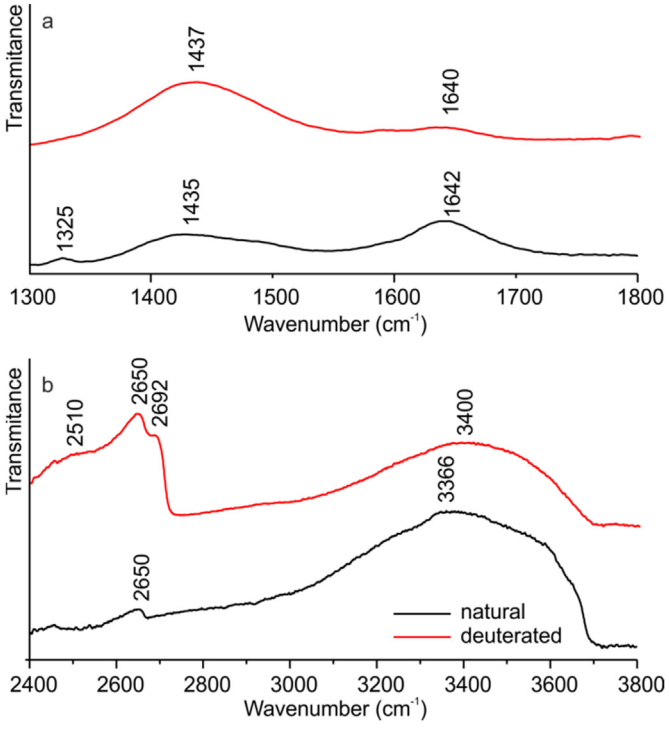

Fig. 6. FTIR spectra of bending (a) and stretching (b) vibration regions in natural and deuterated afwillite.

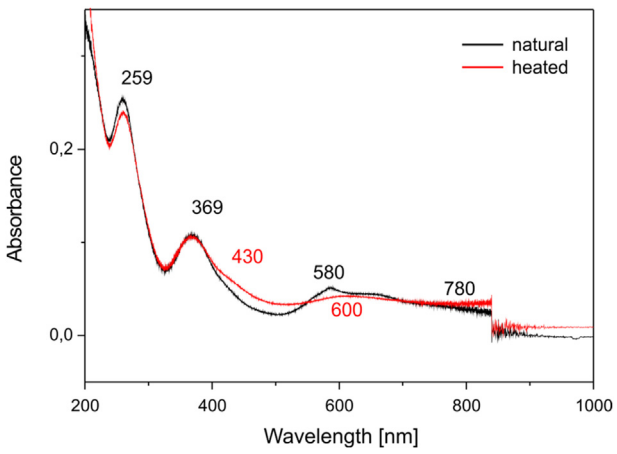

Fig. 7. Absorption spectra of primary and heated afwillite.

ultraviolet range, two absorption bands at 259 nm (4.78 eV) and 369 nm (3.35 eV) were measured. The half-width of the first band is 3750 cm^{-1}, while the second is a little bit less means 3281 cm^{-1}. In far UV the absorption edge at 221 nm (5.60 eV) was recorded. For the heated sample, we observe the change of maximum band position. It can be noticed, however, that from the longer waves of the 369 nm band pronounced shoulder at 430 nm (2.86 eV) appeared. In visible region weak and broad absorption band within 580-780 nm (2.13 - 1.58 eV) was measured. The maximum of this band, as well as maximum of transmission, shifted to the longer wavelength for a heated sample. As a result, the original blue-green colour of the sample changed to green. Of course, in pastel shades, i.e. with little colour saturation.

The absorption bands peaked at 259 nm and 369 nm are associated with the hole oxygen defect, most probably SiO_3^- [46,47]. This hole defects can be associated with a certain number of Ca-vacancies, or Ca^{2+} shifted to other lattice sites. These vacancies or defects can form clusters, as in some fluorite CaF_2 species. There is a known case of *M*-centres, i.e. two conjugated *F*-centres which changed their size under the effect of heating and irradiation and caused the change the fluorite colour. It was proposed [48] than in Ca clusters with 1 nm in size, the absorption band falls within the range of 2.3 eV, i.e. 536 nm. It was recognized as the band from the centre of *M*. For this reason, some changes in the size of the cluster could take some Si-O or Si-OH bonds may have changed, most likely these are shortened. Consequently, a certain modification of the energy levels of the absorption centres occurs, i.e. an additional band at 430 nm could appear. Absorption in the range 580-780 nm does not originate from electron levels, because no luminescence was measured at the energy of excitation corresponding to these wavelengths. It is caused by light scattering on the clusters of these defects. As a result of the heating, the size of these clusters may change. Therefore, it is possible to recognize this absorption in the 600–800 nm range place and some, ineffective changes in absorption could follow them.

Under continuous excitation at 259 nm and 369 nm, the emission band at 468 nm (2.65 eV) was measured. The luminescence intensity for $\lambda_{exc} = 369$ nm and was three times weaker than for $\lambda_{exc} = 259$ nm (Fig. 8a). For the heated sample, the maximum of emission was shifted to longer wavelengths in relation to the position of the unheated sample (Fig. 8b). The difference in energy is

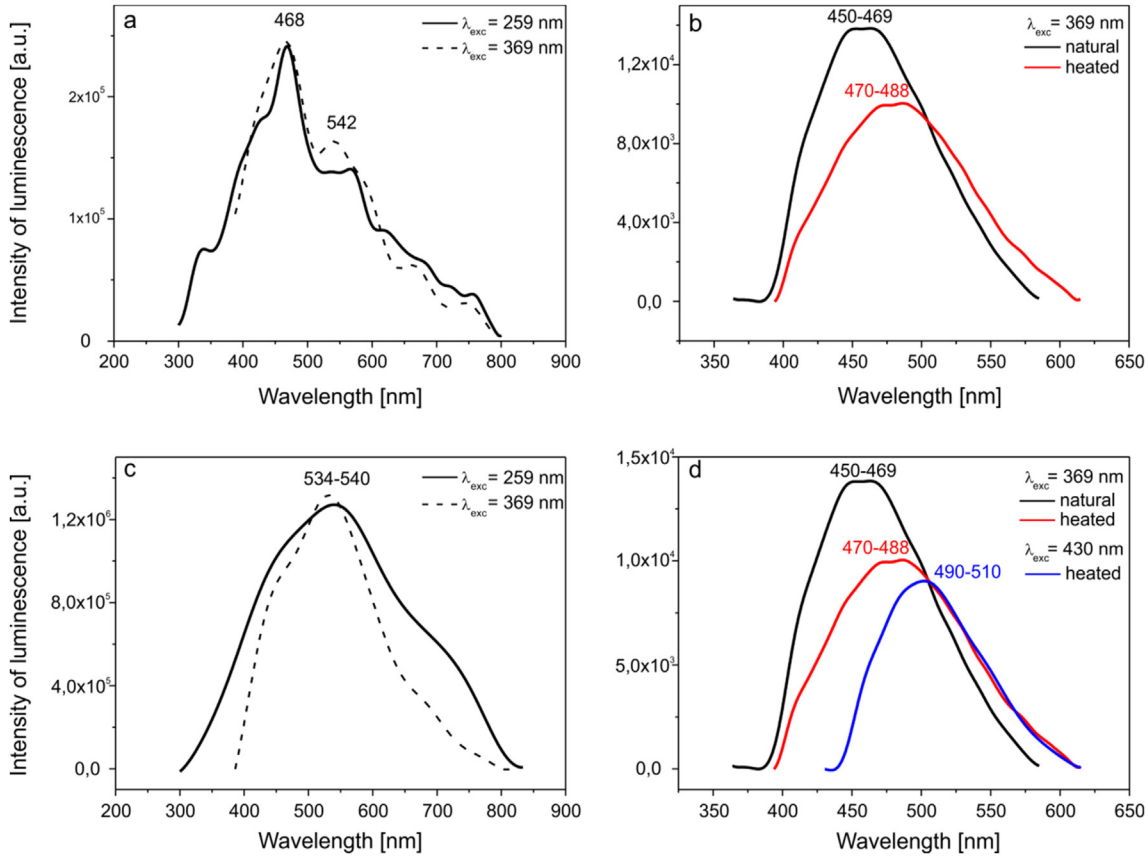

Fig. 8. Photoluminescence spectra of afwillite: a) for continuous excitation $\lambda = 259$ nm and $\lambda = 369$ nm (intensity multiplied by 3); b) with ultra-short excitation for natural and heated sample: c) for heated sample and continuous excitation $\lambda = 259$ nm and $\lambda = 369$ nm (intensity multiplied by 7); d) for natural and heated sample with ultra-short excitation $\lambda = 369$ nm and $\lambda = 430$ nm (intensity multiplied by 8).

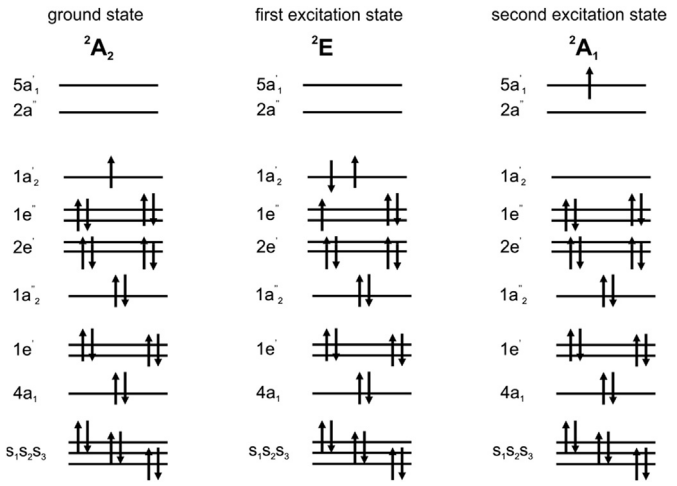

Fig. 9. Molecular orbitals scheme for SiO_3^{3-} radical, modified after Marfunin [52].

rather significant i.e., 0.327 eV. Now the intensity of luminescence for $\lambda_{exc} = 369$ nm is 7 times weaker than for excitation at 259 nm (Fig. 8c). During ultra-short laser excitation, the luminescence spectrum has been measured for the natural sample only for $\lambda_{exc} = 369$ nm, but no luminescence was obtained for $\lambda_{exc} = 259$ nm. Similar, for the heated sample the luminescence spectra with the femtosecond excitation have been measured only for excitation at 369 nm and 430 nm (Fig. 8d). The intensity of luminescence for excitation at 430 nm was 8 times lower than for excitation at 369 nm. It is related to both types of defect. The luminescence decay time was measured only under ultra-short laser excitation for $\lambda_{exc} = 369$ nm and it was equal to 2.8 ns.

The absorption and emission bands of the studied afwillite are caused by the electron transitions of the hole centre SiO_3^{3-}. The absorption and luminescence are similar to alkali silicate glasses [49] but quite different from defects in silica [50,51]. The scheme of molecular orbitals of this radical after Marfunin [52] is presented in Fig. 9. The ground state is $^2A_2$ with electron configuration $(s_1s_2s_3)^6 (4a_1)^2(1e')^4(1a''_2)^2(2e')^4(1e'')^4 (1a'_2)^1$. The first excited state is ^2E, with configuration $(s_1s_2s_3)^6 (4a_1)^2(1e')^4(1a''_2)^2(2e')^4(1e'')^3 (1a'_2)^2$. The second excitation state is $^2A_1$ with configuration $(s_1s_2s_3)^6 (4a_1)^2(1e')^4(1a''_2)^2(2e')^4(1e'')^4 (1a'_2)^0 (2a'')^0 (5a'_1)^1$. Of course, the energy of the electron transition $^2A_2 \rightarrow {}^2E$ should be lower than of $^2A_2 \rightarrow {}^2A_1$. The electron transition $^2A_2 \rightarrow {}^2E$ is forbidden due to the incompatibility of symmetry, contrary to the second possible transition $^2A_2 \rightarrow {}^2A_1$. Therefore, the absorbance of the first transition should be lower than for $^2A_2 \rightarrow {}^2A_1$ transition. Additionally, the luminescence decay time for $^2E \rightarrow {}^2A_2$ emission should be longer than of $^2A_1 \rightarrow {}^2A_2$. It means that absorption band at 259 nm corresponds to $^2A_1 \rightarrow {}^2A_2$, while absorption bands 369 (and 430 nm for heated sample) – to $^2A_2 \rightarrow {}^2E$ transition. The rate of emission $^2A_1 \rightarrow {}^2A_2$ is very short, so emission is measurable only for continuous excitation, but not under ultra-short excitation.

4. Conclusions/summary

Based on the obtained results the following conclusions can be listed:

1. The blue colour of afwillite crystals from Ma'ale Adummim locality came from the hole oxygen defect, most probably SiO_3^{3-}, which can be associated also with a certain number of Ca-vacancies, Ca or their shifting to other lattice sites. As a result of the heating experiment, the blue colour of afwillite crystals transforms into pastel green at 250 °C.
2. The SC-XRD investigations confirm a presence of the $(SiO_3OH)^{3-}$ units linked among themselves by the hydrogen bond system, which is responsible for structural stability. The presence of $(SiO_3OH)^{3-}$ unit can cause a decreasing symmetry of ideal tetrahedral coordination from T_d to C_{3v}, which implicate the local structural re-arrangement.
3. For the first time, the assignment and interpretation of Raman bands were performed. The Raman spectrum for natural afwillite revealed a great number of bands in the range 780 and 970 cm^{-1}, which can confirm previously assumption about structural deformation enforced by protonation of the ideal silica tetrahedron. Another hypothesis explaining observed effects is the presence of two different kinds of structural units: $(SiO_3OH)^{3-}$ and its deprotonated counterpart $(SiO_4)^{4-}$.
4. The changes observed in the heated Raman spectrum are mainly connected with bands attributed to the $(SiO_3OH)^{3-}$ unit. The bands were reduced and shifted to the lower wavenumbers. Some of them disappeared as a result of distracted hydrogen bonds related to the protonated silica tetrahedron.
5. The interpretation of bands in the infrared and Raman spectra is comparable with respect to bands associated with the Si-O stretching and bending vibration of (SiO_3OH) tetrahedra. We concluded, that the absorption bands over 2300 cm^{-1} corresponding to the stretching vibrations (υ OH) of the OH or H_2O groups, depends on the strength of the hydrogen bond in the crystal structure.

Declaration of competing interest

The authors declare that they have no known competing financial interests or personal relationships that could have appeared to influence the work reported in this paper.

Acknowledgements/Funding

Investigations presented in this paper were supported by the National Science Centre (NCN) of Poland, grant no. 2016/23/N/ST10/00142 (J.R) and by OeAD, CEEPUS CIII-RO-0038, ICM-2018-12254 (R.J.). R.J. would like to thank Mateusz Dulski for the help of interpretation and discussion on Raman spectroscopy and dr Yevgeny Vapnik for the afwillite samples. The authors also thank the anonymous reviewers for their useful and constructive comments, which allowed to improve a previous version of the manuscript.

Appendix A. Supplementary data

Supplementary data to this article can be found online at https://doi.org/10.1016/j.saa.2019.117688.

References

[1] J. Parry, F.E. Wright, Afwillite, a new hydrous calcium silicate, from Dutoitspan mine, Kimberley, South Africa, Mineral. Mag. J. Mineral Soc. 20 (1925) 277–286, https://doi.org/10.1180/minmag.1925.020.108.02.
[2] G. Switzer, E.H. Bailey, Afwillite from Crestmore, California, Am. Mineral. 38 (1953) 629–633.
[3] I. Kusachi, C. Henmi, K. Henmi, Afwillite and jennite from Fuka, okayama prefecture, Japan, Mineral. J. 14 (1989) 279–292, https://doi.org/10.2465/minerj.14.279.
[4] R.K. Rastsvetaeva, N.V. Chukanov, A.E. Zadov, Refined structure of afwillite from the Northern Baikal region, Crystallogr. Rep. 54 (2009) 418–422, https://doi.org/10.1134/S1063774509030080.
[5] F. Stoppa, F. Scordari, E. Mesto, V.V. Sharygin, G. Bortolozzi, Calcium-aluminum-silicate-hydrate "cement" phases and rare Ca-zeolite association at Colle Fabbri, Central Italy, Cent. Eur. J. Geosci. 2 (2010) 175–187, https://doi.org/10.2478/v10085-010-0007-6.
[6] H.D. Megaw, The structure of afwillite, $Ca_3(SiO_3OH)_2 \cdot 2H_2O$, Acta Crystallogr. 5 (1952) 477–491, https://doi.org/10.1107/S0365110X52001404.
[7] K.M.A. Malik, J.W. Jeffery, A re-investigation of the structure of afwillite, Acta Crystallogr. B 32 (1976) 475–480, https://doi.org/10.1107/S0567740876003270.

[8] K.M. Moody, The thermal decomposition of afwillite, Mineral. Mag. J. Mineral Soc. 29 (1952) 838–840, https://doi.org/10.1180/minmag.1952.029.216.05.

[9] R.W. Davis, J.F. Young, Hydration and strength development in tricalcium silicate pastes seeded with afwillite, J. Am. Ceram. Soc. 58 (1975) 67–70, https://doi.org/10.1111/j.1151-2916.1975.tb18987.x.

[10] M. Horgnies, L. Fei, R. Arroyo, J.J. Chen, E.M. Gartner, The effects of seeding C_3S pastes with afwillite, Cement Concr. Res. 89 (2016) 145–157, https://doi.org/10.1016/j.cemconres.2016.08.015.

[11] C.E. Tilley, An association of afwillite with spurrite, Geol. Mag. 67 (1930) 168–169, https://doi.org/10.1017/S0016756800099143.

[12] L. Heller, H.F.W. Taylor, Hydrated calcium silicates. Part IV. Hydrothermal reactions: lime : silica ratios 2 : 1 and 3 : 1, J. Chem. Soc. (1952) 2535–2541, https://doi.org/10.1039/JR9520002535.

[13] V. Petříček, M. Dušek, L. Palatinus, Crystallographic computing system JANA2006: general features, Z. für Kristallogr. - Cryst. Mater. 229 (2014) 345–352, https://doi.org/10.1515/zkri-2014-1737.

[14] Y.K. Bentor, S. Gross, L. Heller, Some unusual minerals from the "Mottled Zone" complex, Israel, American Mineralogist 48 (1963) 924–930.

[15] S. Gross, The Mineralogy of the the Hatrurim Formation, Israel, Geological Survey of Israel, 1977.

[16] A. Burg, A. Starinsky, Y. Bartov, Y. Kolodny, Geology of the Hatrurim formation ("Mottled Zone") in the Hatrurim basin, Isr. J. Earth Sci. 40 (1991) 107–124.

[17] I. Techer, H.N. Khoury, E. Salameh, F. Rassineux, C. Claude, N. Clauer, M. Pagel, J. Lancelot, B. Hamelin, E. Jacquot, Propagation of high-alkaline fluids in an argillaceous formation: case study of the Khushaym Matruk natural analogue (Central Jordan), J. Geochem. Explor. 90 (2006) 53–67, https://doi.org/10.1016/j.gexplo.2005.09.004.

[18] E. Sokol, I. Novikov, S. Zateeva, Ye Vapnik, R. Shagam, O. Kozmenko, Combustion metamorphism in the Nabi Musa dome: new implications for a mud volcanic origin of the Mottled Zone, Dead Sea area, Basin Res. 22 (2010) 414–438, https://doi.org/10.1111/j.1365-2117.2010.00462.x.

[19] Y.I. Geller, A. Burg, L. Halicz, Y. Kolodny, System closure during the combustion metamorphic "Mottled Zone" event, Israel, Chemical Geology 334 (2012) 25–36, https://doi.org/10.1016/j.chemgeo.2012.09.029.

[20] I. Novikov, Y. Vapnik, I. Safonova, Mud volcano origin of the mottled Zone, South levant, Geosci. Front. 4 (2013) 597–619, https://doi.org/10.1016/j.gsf.2013.02.005.

[21] I.O. Galuskina, Y. Vapnik, B. Lazic, T. Armbruster, M. Murashko, E.V. Galuskin, Harmunite $CaFe_2O_4$: a new mineral from the jabel harmun, west bank, Palestinian Autonomy, Israel, Am. Mineral. 99 (2014) 965–975, https://doi.org/10.2138/am.2014.4563.

[22] I.O. Galuskina, E.V. Galuskin, A.S. Pakhomova, R. Widmer, T. Armbruster, B. Krüger, E.S. Grew, Y. Vapnik, P. Dzierżanowski, M. Murashko, Khesinite, $Ca_4Mg_2Fe^{3+}{}_{10}O_4[(Fe^{3+}{}_{10}Si_2)O_{36}]$, a new rhönite-group (sapphirine supergroup) mineral from the Negev Desert, Israel– natural analogue of the SFCA phase, Eur. J. Mineral. (2017) 101–116, https://doi.org/10.1127/ejm/2017/0029-2589.

[23] E.V. Galuskin, F. Gfeller, I.O. Galuskina, A. Pakhomova, T. Armbruster, Y. Vapnik, R. Włodyka, P. Dzierżanowski, M. Murashko, New minerals with a modular structure derived from hatrurite from the pyrometamorphic Hatrurim Complex. Part II. Zadovite, $BaCa_6[(SiO_4)(PO_4)](PO_4)_2F$ and aradite, $BaCa_6[(SiO_4)(VO_4)](VO_4)_2F$, from paralavas of the Hatrurim Basin, Negev Desert, Israel, Mineral. Mag. 79 (2015) 1073–1087, https://doi.org/10.1180/minmag.2015.079.5.04.

[24] E.V. Galuskin, F. Gfeller, I.O. Galuskina, T. Armbruster, A. Krzątała, Y. Vapnik, J. Kusz, M. Dulski, M. Gardocki, A.G. Gurbanov, P. Dzierżanowski, G.D. Gatta, New minerals with a modular structure derived from hatrurite from the pyrometamorphic rocks. Part III. Gazeevite, $BaCa_6(SiO_4)_2(SO_4)_2O$, from Israel and the Palestine Autonomy, South levant, and from South ossetia, greater Caucasus, Mineral. Mag. 81 (2017) 499–513, https://doi.org/10.1180/minmag.2016.080.105.

[25] E.V. Galuskin, B. Krüger, I.O. Galuskina, H. Krüger, Y. Vapnik, J.A. Wojdyla, M. Murashko, New mineral with modular structure derived from hatrurite from the pyrometamorphic rocks of the Hatrurim complex: ariegilatite, $BaCa_{12}(SiO_4)_4(PO_4)_2F_2O$, from negev Desert, Israel, Minerals 8 (2018) 109, https://doi.org/10.3390/min8030109.

[26] E.V. Sokol, Y.V. Seryotkin, S.N. Kokh, Y. Vapnik, E.N. Nigmatulina, S.V. Goryainov, E.V. Belogub, V.V. Sharygin, Flamite, (Ca,Na,K)2(Si,P)O4, A new mineral from ultrahightemperature combustion metamorphic rocks, Hatrurim Basin, Negev Desert, Israel, Mineralogical Magazine 79 (2015) 583–596, https://doi.org/10.1180/minmag.2015.079.3.05.

[27] H.N. Khoury, E.V. Sokol, S.N. Kokh, Y.V. Seryotkin, E.N. Nigmatulina, S.V. Goryainov, E.V. Belogub, I.D. Clark, Tululite, $Ca_{14}(Fe^{3+},Al)(Al,Zn,Fe^{3+},Si,P,Mn,Mg)_{15}O_{36}$: a new Ca zincate-aluminate from combustion metamorphic marbles, central Jordan, Miner Petrol 110 (2016) 125–140, https://doi.org/10.1007/s00710-015-0413-3.

[28] S.N. Britvin, Y. Vapnik, Y.S. Polekhovsky, S.V. Krivovichev, M.G. Krzhizhanovskaya, L.A. Gorelova, O.S. Vereshchagin, V.V. Shilovskikh, A.N. Zaitsev, Murashkoite, FeP, a new terrestrial phosphide from pyrometamorphic rocks of the Hatrurim Formation, South Levant, Miner Petrol 113 (2019) 237–248, https://doi.org/10.1007/s00710-018-0647-y.

[29] K. Robinson, G.V. Gibbs, P.H. Ribbe, Quadratic elongation: a quantitative measure of distortion in coordination polyhedra, Science 172 (1971) 567–570, https://doi.org/10.1126/science.172.3983.567.

[30] E. Libowitzky, Correlation of O-H stretching frequencies and O-H···O hydrogen bond lengths in minerals, Monatshefte Fuer Chemie 130 (1999) 1047–1059, https://doi.org/10.1007/BF03354882.

[31] R.L. Frost, J. Čejka, M.L. Weier, W. Martens, Molecular structure of the uranyl silicates—a Raman spectroscopic study, J. Raman Spectrosc. 37 (2006) 538–551, https://doi.org/10.1002/jrs.1430.

[32] G. Spiekermann, M. Steele-MacInnis, C. Schmidt, S. Jahn, Vibrational mode frequencies of silica species in SiO_2-H_2O liquids and glases from ab initio molecular dynamics, J. Chem. Phys. 136 (2012) 154501, https://doi.org/10.1063/1.3703667.

[33] M. Dulski, A. Bulou, K.M. Marzec, E.V. Galuskin, R. Wrzalik, Structural characterization of rondorfite, calcium silica chlorine mineral containing magnesium in tetrahedral position $[MgO_4]^{6-}$, with the aid of the vibrational spectroscopies and fluorescence, Spectrochim. Acta A Mol. Biomol. Spectrosc. 101 (2013) 382–388, https://doi.org/10.1016/j.saa.2012.09.090.

[34] W. Pilz, Raman spectra of silicates, Acta Phys. Hung. 61 (1987) 27–30, https://doi.org/10.1007/BF03053810.

[35] M. Handke, M. Urban, IR and Raman spectra of alkaline earth metals orthosilicates, J. Mol. Struct. 79 (1982) 353–356, https://doi.org/10.1016/0022-2860(82)85083-7.

[36] P. McMillan, Structural studies of silicate glasses and melts—applications and limitations of Raman spectroscopy, Am. Mineral. 69 (1984) 622–644.

[37] K.N. Dalby, P.L. King, A new approach to determine and quantify structural units in silicate glasses using micro-reflectance Fourier-Transform infrared spectroscopy, Am. Mineral. 91 (2015) 1783–1793, https://doi.org/10.2138/am.2006.2075.

[38] W.P. Griffith, Raman studies on rock-forming minerals. Part I. Orthosilicates and cyclosilicates, J. Chem. Soc. A. (1969) 1372–1377, https://doi.org/10.1039/J19690001372.

[39] C. Biagioni, E. Bonaccorsi, S. Merlino, Crystal structure of bultfonteinite, $Ca_4[SiO_3(OH)]_2F_2 \cdot 2H_2O$, from N'chwaning II mine (kalahari manganese field, republic of South Africa)., atti della società toscana di scienze naturali, Memorie, Serie A (2010) 9–15.

[40] P. Bonazzi, L. Bindi, O. Medenbach, R. Pagano, G.I. Lampronti, S. Menchetti, Olmiite, $CaMn[SiO_3(OH)](OH)$, the Mn-dominant analogue of poldervaartite, a new mineral species from Kalahari manganese fields (Republic of South Africa), Mineral. Mag. 71 (2007) 193–201, https://doi.org/10.1180/minmag.2007.071.2.193.

[41] Y. Dai, G.E. Harlow, A.R. McGhie, Poldervaartite, $Ca(Ca_{0.5}Mn_{0.5})(SiO_3OH)(OH)$, a new acid nesosilicate from the Kalahari manganese field, South Africa: crystal structure and description, Am. Mineral. 78 (1993) 1082–1087.

[42] R.L. Frost, R. Scholz, A. López, Y. Xi, A. Granja, Ž. Žigovečki Gobac, R.M.F. Lima, Infrared and Raman spectroscopic characterization of the silicate mineral olmiite $CaMn^{2+}[SiO_3(OH)](OH)$ – implications for the molecular structure, J. Mol. Struct. 1053 (2013) 22–26, https://doi.org/10.1016/j.molstruc.2013.08.038.

[43] R.L. Frost, A. López, R. Scholz, R.M.F. Lima, Vibrational spectroscopic study of poldervaartite $CaCa[SiO_3(OH)(OH)]$, Spectrochim. Acta A Mol. Biomol. Spectrosc. 137 (2015) 827–831, https://doi.org/10.1016/j.saa.2014.09.017.

[44] H.E. Petch, N. Sheppard, H.D. Megaw, The infra-red spectrum of afwillite, $Ca_3(SiO_3OH)_2 \cdot 2H_2O$, in relation to the proposed hydrogen positions, Acta Crystallogr. 9 (1956) 29–34, https://doi.org/10.1107/S0365110X5600005X.

[45] N.V. Chukanov, Infrared Spectra of Mineral Species: Extended Library, Springer Netherlands, 2014. https://www.springer.com/gp/book/9789400771277. (Accessed 29 August 2019). accessed.

[46] null Stashans, null Kotomin, null Calais, Calculations of the ground and excited states of F-type centers in corundum crystals, Phys. Rev. B Condens. Matter 49 (1994) 14854–14858, https://doi.org/10.1103/physrevb.49.14854.

[47] A.F. Zatsepin, V.B. Guseva, D.A. Zatsepin, Luminescence of modified non-bridging oxygen hole centers in silica and alkali silicate glasses, Glass Phys. Chem. 34 (2008) 709–715, https://doi.org/10.1134/S1087659608060084.

[48] L.E. Murr, Ordered lattice defects in colored fluorite: direct observations, Science 183 (1974) 206–208, https://doi.org/10.1126/science.183.4121.206.

[49] K. Przibram, Colour bands in fluorspar, Nature 172 (1953) 860–861, https://doi.org/10.1038/172860b0.

[50] L. Skuja, Optically active oxygen-deficiency-related centers in amorphous silicon dioxide, J. Non-Cryst. Solids 239 (1998) 16–48, https://doi.org/10.1016/S0022-3093(98)00720-0.

[51] G. Pacchioni, A.M. Ferrari, G. Ieranò, Cluster Model Calculations of Oxygen Vacancies in SiO_2 and MgO Formation Energies, optical transitions and EPR spectra, 1997, https://doi.org/10.1039/a701361b.

[52] A.S. Marfunin, Spectroscopy, Luminescence and Radiation Centers in Minerals, Springer-Verlag, Berlin Heidelberg, 1979. https://www.springer.com/gp/book/9783642671142. (Accessed 29 August 2019). accessed.